The 17th Annual IEEE International Symposium on Personal, Indoor and Mobile Radio Communications (PIMRC'06)

MIMO UWB COMMUNICATIONS USING MODIFIED HERMITE PULSES

Chadi Abou-Rjeily, Norbert Daniele
Laboratory of Electronics and Information Technology
CEA-LETI, 17 rue des Martyrs, 38054 Grenoble
France
{chadi.abourjeily, norbert.daniele}@cea.fr

Jean-Claude Belfiore
École Nationale Supérieure des Télécommunications
ENST, 46 rue Barrault, 75013 Paris
France
belfiore@enst.fr

ABSTRACT

In this paper, we present a new full rate scheme for exploiting diversity in multi-antenna ultra-wideband (UWB) systems. The independent data streams that are transmitted simultaneously from the different antennas are rendered orthogonal by the use of modified Hermite pulses. At a second time, appropriate real rotations enhance the transmit diversity level. We also consider, for the first time, the problem of Maximum Likelihood (ML) detection with multi-dimensional PPM and hybrid PPM-PAM constellations that can be used in conjunction with the proposed scheme.

I. INTRODUCTION

A large number of full rate and fully diverse space-time (ST) codes was proposed in the literature [1–3]. However, all of these ST codes are complex-valued and hence not adapted to real carrier-less impulse radio ultra-wideband (IR-UWB) that can not support phase rotations. The necessity of having real-valued transmissions constitutes a very limiting constraint. In fact, all multiple input multiple output (MIMO) UWB schemes proposed in the literature focused on increasing the data rate [4–6] or enhancing the diversity [7] separately. Totally-real constructions for UWB systems were proposed in [8] where an amplitude amplification (rather than a phase rotation) permitted to achieve full diversity. The introduction of non-unitary coefficients in the codewords results in some performance losses as noted in [3]. This was remedied in [8] by taking advantage of the pulse repetitions used to convey each information symbol in time hopping (TH) UWB. The limitation is that very high data rate systems may not employ any repetitions.

On the other hand, the Hermite pulses are well known in the literature of UWB. They were used in single antenna systems to increase the data rate by transmitting several pulses with different orders simultaneously [9, 10]. A similar approach is used in [5,6] with multi-antenna systems where two orthogonal pulses used for the channel estimation and data transmissions are transmitted simultaneously.

In this paper, in order to overcome the constraint imposed by totally real transmissions, we propose a new diversity scheme that is based on modified Hermite pulses used in conjunction with modulation diversity [11]. For a system equipped with P transmit antennas, an appropriate rotation is applied on the information symbols mapped on the P orthogonal signal subspaces. The proposed system is associated with one-dimensional pulse amplitude modulation (PAM), multi-dimensional pulse position modulation (PPM) and hybrid PPM-PAM. Performance is analyzed over realistic UWB channels [12] where multi-path components arriving within the same pulse duration can reduce the level of orthogonality at the receiver side.

Another issue addressed in this paper is the problem of Maximum Likelihood (ML) detection with multi-dimensional (PPM-PAM or PPM) constellations. These constellations are sparse and the different components of the transmitted information vectors are not independent. We propose non-trivial modifications of the sphere decoder [13], [14]. This avoids the convergence towards a non-valid point and enhances the convergence time.

The rest of the paper is organized as follows. Section II describes the system model of the proposed MIMO-UWB scheme. The decoding algorithms are given in section III. Simulations over highly frequency selective channels are presented in section IV while section V concludes.

II. SYSTEM MODEL

In hybrid M-PPM and M'-PAM, the input data is modulated onto both the pulse amplitudes and pulse positions. Each element of this constellation is represented by a M-dimensional vector that belongs to the set:

$$\mathcal{C}=\{(2m'-1-M')e_{m+1}; m'=1,\ldots,M'; m=0,\ldots,M-1\} \quad (1)$$

where e_m is the m-th column of the $M \times M$ identity matrix I_M. PPM and PAM follow as special cases.

For a MIMO-UWB system with P transmit and Q receive antennas, the pulse shaper at the p-th antenna is chosen to be the modified Hermite polynomial of order p [9]:

$$w_p(t) = (-1)^p \exp\left(\frac{t^2}{4\Gamma}\right) \frac{\mathrm{d}^p}{\mathrm{d}t^p}\left(\exp\left(-\frac{t^2}{2\Gamma}\right)\right) \quad (2)$$

where Γ regulates the width of the pulses and it is chosen to be independent from p. This choice implies that higher order pulses will have larger durations but the orthogonality between the P pulses is conserved. Multiplying eq. (2) by a sinusoidal waveform along with an appropriate choice of Γ [10] results in pulses respecting the FCC mask.

For single user TH-UWB systems, the signal transmitted from the p-th transmit antenna can be expressed as:

$$s_p(t) = \frac{1}{\sqrt{PN_f}} \sum_{n=0}^{N_f-1} \sum_{m=0}^{M-1} s_{p,m} w_p(t - nT_f - m\delta) \quad (3)$$

where normalizing by P insures the same total transmitted energy as in the single-antenna case. N_f pulses with different

1-4244-0330-8/06/$20.00

time shifts are used to convey each information symbol. Each one of these pulses is emitted during a time frame of duration T_f resulting in a data rate of $P\log_2(MM')/T_s$ bits/s where $T_s = N_f T_f$ is the symbol duration. δ is the modulation delay. In order to eliminate Inter Symbol Interference (ISI), T_f is chosen to be larger than the channel delay spread. $s_{p,m}$ is the $(m+1)$-th component of vector S_p for $m = 0, \ldots, M-1$ and $p = 1, \ldots, P$. These vectors are related to the information vectors $A_1, \ldots, A_P \in \mathcal{C}$ by:

$$[S_1^T \ \cdots \ S_P^T]^T = (\mathcal{R} \otimes I_M)[A_1^T \ \cdots \ A_P^T]^T \tag{4}$$

where $\otimes$ stands for the Kronecker product and $\mathcal{R}$ is any fully diverse $P \times P$ rotation matrix [11]. In eq. (4), a rotation is applied between the m-th components of the P information symbols. After that, the rotated components are transmitted over the P signal subspaces determined by the different pulse forms. This strategy is similar to those applied in [1, 8] where, at a first time, rotations are applied between the P components of each layer of the codewords. At a second time, these layers are rendered orthogonal to each other by an appropriate choice of an algebraic or transcendental element. In our case, we take advantage of the impulsive nature of the transmitted signals in order to introduce orthogonality by the use of modified Hermite pulses.

The received signal at the q-th antenna takes the form:

$$r_q(t) = \frac{1}{\sqrt{PN_f}} \sum_{p,n,m} s_{p,m} h_{q,p}(t - nT_f - m\delta) + n_q(t) \tag{5}$$

where $n_q(t)$ is the noise at the q-th antenna which is real AWGN with double sided spectral density $N_0/2$. $h_{q,p}(t) = w_p(t) * h'_{q,p}(t)$ where $*$ stands for convolution and $h'_{q,p}(t)$ is the impulse response of the frequency selective channel between the p-th transmit and the q-th receive antenna.

A Rake with order L is used after each receive antenna. For a given finger delay, the received signal corresponding to the m-th position is projected on the P signal subspaces. The decision variables at the receiver are given by:

$$x_{q,l,p,m} = \int_0^{T_s} r_q(t) \tilde{w}_{l,p,m}(t) \mathrm{d}t \tag{6}$$

$$= \sqrt{\frac{N_f}{P}} \sum_{p',m'} s_{p',m'} h_{q,p,p'}((m-m')\delta + \Delta_l) + n_{q,l,p,m} \tag{7}$$

where $h_{q,p,p'}(\tau) = \int_0^{T_f} h_{q,p'}(t) w_p(t-\tau) \mathrm{d}t$. The LPM reference signals in eq. (6) are given by:

$$\tilde{w}_{l,p,m}(t) = \sum_{n=0}^{N_f-1} w_p(t - nT_f - \Delta_l - m\delta) \tag{8}$$

where Δ_l is the l-th finger delay. We fix $\Delta_l = lMT_w$ for $l = 0, \ldots, L-1$ where T_w is the pulse width of $w_P(t)$ which has the largest duration. It is easy to show that this choice of Δ_l along with $\delta \geq T_w$ result in white noise terms $n_{q,l,p,m}$.

Equation (7) can be expressed in matrix form as:

$$X = H(\mathcal{R} \otimes I_M)A + N \tag{9}$$

where X is the vertical concatenation of $x_{q,l,p,m}$. N is a white noise vector with variance $\frac{PN_0}{2}$ and it is constructed in the same way as X. A is the vertical concatenation of $A_1, \ldots, A_P$. $H = [H_1^T, \ldots, H_Q^T]^T$ where $H_q = [H_{q,0}^T, \ldots, H_{q,L-1}^T]^T$ is a $LPM \times PM$ matrix corresponding to the q-th receive antenna. The $PM \times PM$ matrix $H_{q,l}$ takes the form:

$$H_{q,l} = \begin{bmatrix} H_{q,l,1,1} & \cdots & H_{q,l,1,P} \\ \vdots & \ddots & \vdots \\ H_{q,l,P,1} & \cdots & H_{q,l,P,P} \end{bmatrix} \tag{10}$$

where the (m, m')-th element of the constituent $M \times M$ matrix $H_{q,l,p,p'}$ is equal to $h_{q,p,p'}((m-m')\delta + \Delta_l)$.

The proposed system will be referred to as coded system in what follows. The term uncoded systems is reserved to spatial multiplexing. In other words $w_p(t)$ has the same form for all values of p and the matrix $\mathcal{R}$ in eq. (9) is replaced by I_P. For uncoded systems, LM matched filters are employed after each receive antenna resulting in QLM decision variables. In this case, $H_{q,l}$ in eq. (10) reduces to the horizontal concatenation of $H_{q,l,p,p}$ for $p = 1, \ldots, P$.

With respect to uncoded and ST-coded [8] MIMO systems, the proposed scheme deploys $QLPM$ rather than QLM matched filters. Moreover, the estimation of the channel matrix necessitates the estimation of QLP^2M rather than $QLPM$ parameters as in uncoded and ST-coded systems. However, with respect to minimal-delay, full rate and fully diverse ST codes, the proposed system has a lower decoding complexity that grows with P rather than P^2. With respect to uncoded systems, the proposed scheme presents the advantage of an enhanced transmit diversity with the same decoding complexity. It is interesting to compare coded systems having L fingers with uncoded systems having PL fingers since in this case the number of matched filters, decoding complexity and the data rate are the same.

Because of the highly frequency selective UWB channel, multi-path components can arrive within the same pulse duration. This implies that the orthogonality is only partial at the receiver side. Despite this, we show later through simulations that the better conditioned channel matrix results in better performance. Moreover, the modulation diversity turns out to be robust against the mixing, caused by the channel, between the coordinates of the coded symbols that are mapped onto the different signal subspaces.

III. Sphere decoder

For M-PPM-M'-PAM, the coordinates of the MP-dimensional information vector A in eq. (9) are not independent. Moreover, the generated lattice has a cardinality of $(M'+1)^{MP}$ since the amplitude in each position can be equal to zero in addition to the M' nonzero values. However, among these points only $(MM')^P$ points are valid. Therefore, applying the sphere decoder without any modifications can result in non-valid points. This can be simply remedied by applying a validity test at the end of the algorithm. In this case, if the resulting vector does not belong to the constellation it is not kept and the search is restarted. However, this results

in an additional complexity since the modified algorithm will "zigzag" between a large number of non-valid points before reaching the closest valid point. Moreover, this complexity increases with M and M' since the resulting constellations become sparser.

Denote by Q and R the unitary matrix and the upper triangular matrix (with positive diagonal elements) obtained by performing the QR decomposition on the matrix $H(\mathcal{R} \otimes I_M)$ in eq. (9). Denoting by $z = Q^T X$ a rotated version of the initial decision vector X, the search algorithm is equivalent to finding the point $a \in \mathcal{C}^P$ that minimizes $\|z - Ra\|^2$ where $\|.\|^2$ corresponds to the Frobenius norm.

We propose two versions of the modified multi-dimensional sphere decoder (SD). Both versions are based on the Pohst enumeration strategy [13, 14]. Even though the first version is not the best solution, it is presented for comprehensive reasons and it constitutes an intermediary step for deriving the second algorithm.

The first algorithm is a direct modification of the SD obtained by a continuous adaptation of the boundaries at each level based on the tested points at previous levels. In what follows, the function enum(a, b) enumerates all elements of the set $S = \{0, \pm 1, \ldots, \pm(M' - 1)\}$ that belong to the interval $[a\ b]$. The function length(a, b) returns the number of elements in enum(a, b). The parts of the algorithm that are specific to this extension are written between parenthesis while the remaining parts correspond to the Pohst strategy as can be found in [14] for example.

Step 1: Set $P' = PM$, $i = P'$, $T_{P'} = 0$; $\xi_{P'} = 0$, $flag = \mathrm{O}_{P' \times 1}$, $d = C$ *(sphere squared radius).*

Step 2: If $d < T_i$ *go to Step 4 else* {*If* $flag(i) = 1$ $A_i = B_i = 0$ *else*

$$A_i = \max\left(1 - M', \left\lceil \frac{z_i - \xi_i - \sqrt{d - T_i}}{r_{i,i}} \right\rceil\right)$$

$$B_i = \min\left(M' - 1, \left\lfloor \frac{z_i - \xi_i + \sqrt{d - T_i}}{r_{i,i}} \right\rfloor\right)$$

endif}, $y_i =$ *enum*(A_i, B_i), $N_i =$ *length*(A_i, B_i), $x_i = 0$ *endif.*

Step 3: $x_i = x_i + 1$, *if* $x_i > N_i$ *go to Step 4 else* {*if* $y_i(x_i) \neq 0$, $j = i - 1$ *mod* (M), *for* $k = 1, \ldots, j$ $flag(i - k) = 1$ *endfor elseif* $i = 1$ *mod* (M) *for* $k = i, \ldots, i + M - 1$ $u_k = y_k(x_k)$ *endfor, if* $u = \mathrm{O}_{M \times 1}$ *go to Step 3 endif endif*}, *go to Step 5 endif.*

Step 4: If $i = P'$ *terminate else* $i = i + 1$, {$flag = \mathrm{O}_{P' \times 1}$}, *go to Step 3 endif.*

Step 5: If $i > 1$, $\xi_{i-1} = \sum_{j=i}^{P'} r_{i-1,j}\, y_j(x_j)$, $T_{i-1} = T_i + |z_i - \xi_i - r_{i,i} y_i(x_i)|^2$, *let* $i = i - 1$ *and go to Step 2 endif.*

Step 6: $\hat{d} = T_1 + |z_1 - \xi_1 - r_{1,1} y_1(x_1)|^2$. *If* $\hat{d} < d$ *let* $d = \hat{d}$, *for* $i = 1, \ldots, P'$, $\hat{a}_i = y_i(x_i)$ *endfor endif go to Step 3.*

In the above pseudo-code, $r_{i,j}$ corresponds to the (i, j)-th element of the upper triangular matrix R. $\mathrm{O}_{m \times n}$ corresponds to the $m \times n$ matrix whose elements are equal to 0.

Algorithm 1 is based on the idea that whenever a nonzero coordinate is found (Step 3), the remaining coordinates having smaller indices and corresponding to the nominal positions of the same transmit antenna are set to zero without checking the boundaries of the sphere along these dimensions (Step 2). This follows from the structure of the transmitted information vector A that can be divided into P sub-vectors each consisting of $M - 1$ zeros and one non-zero component that belongs to the M'-PAM constellation. In a similar way, all-zero subvectors are avoided (Step 3). This can be seen as "forcing" the algorithm to zigzag only between valid nodes. This algorithm avoids calculating and spanning many intervals corresponding to the set of valid coordinates. In other words, if a non-zero coordinate is found at the m-th component of a given sub-vector, algorithm 1 "short circuits" the remaining $m - 1$ dimensions at higher levels (levels with smaller indices).

At the i-th level, and for some given values of $a_l \in$ enum(A_l, B_l) for $l = i + 1, \ldots, PM$, algorithm 1 tries to find the set of valid values of a_i verifying:

$$\left| z_i - \sum_{j=i}^{PM} r_{i,j} a_j \right|^2 = |z_i - r_{i,i} a_i - \xi_i|^2 \leq d - T_i \qquad (11)$$

where T_i and ξ_i are updated recursively in the order from PM to 1 and d is changed adaptively along the search (at level 1). We argue that the complexity of algorithm 1 follows from solving eq. (11) over PM dimensions. We propose to group M equations in the form of eq. (11) together and to solve them simultaneously. This is rendered possible because of the structure of the PPM-PAM constellations. These M equations are solved at levels $(p - 1)M + 1$ for $p = P, \ldots, 1$. Grouping the M equations at levels $(p - 1)M + 1, \ldots, pM$, we obtain:

$$\sum_{m=1}^{M} \left| z_m^{(p)} - \sum_{j=f(p,m)}^{PM} r_{f(p,m),j} a_j \right|^2 \leq d - T_p \qquad (12)$$

where $f(p, m) = (p - 1)M + m$ and T is changed recursively after each M levels. $z^{(p)}$ corresponds to the M-dimensional vector composed of the elements $z_{(p-1)M+1}, \ldots, z_{pM}$ of the PM-dimensional vector z. The m-th component of $z^{(p)}$ is denoted by $z_m^{(p)}$. We construct the vectors $a^{(1)}, \ldots, a^{(P)}$ in the same way. As in the preceding algorithm, $r_{i,j}$ is the (i, j)-th element of R.

Given that only one value among $a_{f(p,1)}, \ldots, a_{f(p,M)}$ can be different from zero, determining the boundaries at the level $f(p, m')$ is equivalent to solving (for $m' = 1, \ldots, M$):

$$\sum_{m=1}^{M} \left| z_m^{(p)} - r_{f(p,m),f(p,m')} a_{f(p,m')} - \xi'_{p,m} \right|^2 \leq d - T_p \quad (13)$$

where: $\xi'_{p,m} = \sum_{j=f(p+1,1)}^{PM} r_{f(p,m),j} a_j$.

We introduce the following notations: $a_{m'}^{(p)} = a_{f(p,m')}$ and $R^{(i,j)}$ is the $M \times M$ matrix composed of the elements $r_{m,m'}$ for $m = (i - 1)M + 1, \ldots, iM$ and $m' = (j - 1)M + 1, \ldots, jM$.

Finally, $R^{(i)} = R^{(i,i)}$. The k-th column of a matrix X is denoted by $X_{:,k}$. For a given value of $m' \in \{1, \ldots, M\}$, eq. (12) can be expressed as:

$$\left\| z^{(p)} - a^{(p)}_{m'} R^{(p)}_{:,m'} - \xi_{:,p} \right\|^2 \leq d - T_p \tag{14}$$

where ξ is a $M \times P$ matrix whose p-th column is given by:

$$\xi_{:,p} = \sum_{p'=p+1}^{P} a^{(p')}_{c_{p'}} R^{(p,p')}_{:,c_{p'}} \tag{15}$$

where $c_{p'} \in \{1, \ldots, M\}$ is the position of the pulse transmitted by the p'-th antenna. These values are obtained by back-substitution. The boundaries at the level $(p'-1)M + c_{p'}$ are determined taking into consideration that the amplitudes at levels $(p'-1)M + 1, \ldots, (p'-1)M + c_{p'} - 1, (p'-1)M + c_{p'} + 1, \ldots, p'M$ are all equal to zero. $a^{(p')}_{c_{p'}}$ is allowed to vary between the boundaries at this level.

Step 1: Set $i = P$, $T_i = 0$, $\xi_{:,i} = \mathrm{O}_{M\times 1}$, $d = C$ *(sphere squared radius).*

Step 2: If $d < T_i$ *go to Step 4 else* $f = \left(z^{(i)} - \xi_{:,i}\right)^T \left(z^{(i)} - \xi_{:,i}\right) - d + T_i$, *for* $m = 1, \ldots, M$ $a = R^{(i)T}_{:,m} R^{(i)}_{:,m}$, $b = -R^{(i)T}_{:,m} \left(z^{(i)} - \xi_{:,i}\right)$, $\delta = b^2 - af$. *If* $\delta < 0$ $A^{(i)}_m = B^{(i)}_m = 0$ *else*

$$A^{(i)}_m = \max\left(1 - M', \left\lceil \frac{-b - \sqrt{\delta}}{a} \right\rceil\right)$$

$$B^{(i)}_m = \min\left(M' - 1, \left\lfloor \frac{-b + \sqrt{\delta}}{a} \right\rfloor\right)$$

endif, $x^{(i)}_m = A^{(i)}_m - 2$ *endfor* $c_i = 1$ *endif.*

Step 3: $x^{(i)}_m = x^{(i)}_m + 2$, *if* $x^{(i)}_m > B^{(i)}_m$ *go to Step 4 else go to Step 5 endif.*

Step 4: $c_i = c_i + 1$, *if* $c_i = M + 1$ *if* $i = P$ *terminate else* $i = i + 1$ *endif endif go to Step 3.*

Step 5: If $i > 1$ $\xi_{:,i-1} = \sum_{j=i}^{P} x^{(j)}_{c_j} R^{(i-1,j)}_{:,c_j}$, $T_{i-1} = T_i + \|z^{(i)} - \xi_{:,i} - x^{(i)}_{c_i} R^{(i)}_{:,c_i}\|^2$, $i = i - 1$ *go to Step 2 endif.*

Step 6: $\hat{d} = T_1 + \|z^{(1)} - \xi_{:,1} - x^{(1)}_{c_1} R^{(1)}_{:,c_1}\|^2$. *If* $\hat{d} < d$ *let* $d = \hat{d}$, *for* $p = 1, \ldots, P$ $\hat{a}_p = x^{(p)}_{c_p} I_{:,c_p}$ *endfor endif go to Step 3 (I is the* $M \times M$ *identity matrix).*

Algorithm 2 is the recursive solution of eq. (14). It is equivalent to considering P levels where each level has M sub-levels whose boundaries are determined jointly. Note that there is no need for the function "enum" as in algorithm 1 because the amplitude levels now belong to $\{\pm 1, \ldots, \pm(M'-1)\}$ rather than $\{0, \pm 1, \ldots, \pm(M'-1)\}$.

In order to have reproducible results that are independent from the speed of the simulating machines, the convergence times of the above algorithms are determined with respect to the following algorithm referred to as algorithm 0. It is based on a straight-forward modification of the SD. Besides constituting a relative time reference, it is also presented to show how far the trivial solution is from the proposed algorithms. Algorithm 0 consists of a continuous checking of the validity of each part of the sub-vectors. If the validity test fails, an adjacent node at the same level is checked; if the failure corresponds to the last node at a given level, algorithm 0 passes to a lower dimension (one with a higher index). These modifications correspond to replacing Step 3 in algorithm 1 by:

Step 3: $x_i = x_i + 1$ *if* $x_i \leq N_i$ {*for* $j = i, \ldots, \lceil \frac{i}{M} \rceil M$ *do* $u_j = y_j(x_j)$ *endfor, if validity_test*$(u) = 1$ *go to Step 5 else go to Step 3 endif*} endif.

where the function validity_test assures that a part consisting of m coordinates of a sub-vector contains no more than one nonzero entry and that this part contains exactly one nonzero entry for $m = M$. The disadvantage is that the function validity_test is performed each time we pass from one dimension to another. The complexity is higher than that of the classical SD with PM dimensions.

IV. Simulations and results

The PQ channels between the different antennas are generated according to the channel model recommendation CM2 [12]. The modulation delay is equal to the width of the highest order pulse $\delta = T_{wp} = 0.5$ ns. The frame duration T_f is chosen to be $T_f = 100$ ns which is larger than the maximum delay spread of CM2 [12]. N_f has no effect on the performance in single user situations and it is fixed to 1.

Fig. 1 shows the performance at a rate of 4 bits per channel use (PCU). We fix $P = Q = 4$. The uncoded and coded systems are compared with each other and with the existing UWB diversity schemes in [7] and [8] referred to as "OC" (orthogonal code) and "ST-coded" respectively. The legend "Hermite" stands for the system using modified Hermite pulses with no modulation diversity. In order to achieve the given rate, all schemes use 2-PAM except for the rate-1 code "OC" that must use 16-PAM. Results show the importance of merging the use of modified Hermite pulses with modulation diversity. For example, at an error rate of 10^{-4}, the coded 1-finger system outperforms the uncoded 4-finger system by 2 dB while having the same number of matched filters and decoding complexity. With respect to [8], coded systems use 4 times more correlators but the SD converges 80 times faster at a signal to noise ratio of 15 dB (the initial sphere radius is set to infinity).

Fig. 2 shows the performance with 8-PPM-8-PAM, $P = 3$, $Q = 1$ and $L = 8$ using algorithm 2 and MMSE receivers. MIMO and single-antenna systems transmit at 180 Mbits/s and 60 Mbits/s respectively. Results show that the better conditioned channel matrix that follows from the use of modified Hermite pulses permits linear receivers to close the gap with respect to the optimal detectors.

Fig. 3 compares the complexity of algorithm 1 and algorithm 2 for different hybrid constellation sizes for coded systems with 2 transmit antennas, 2 receive antennas and 1 finger Rake. The ordinate corresponds to the value t_0/t_i for $i = 1, 2$ where t_j is

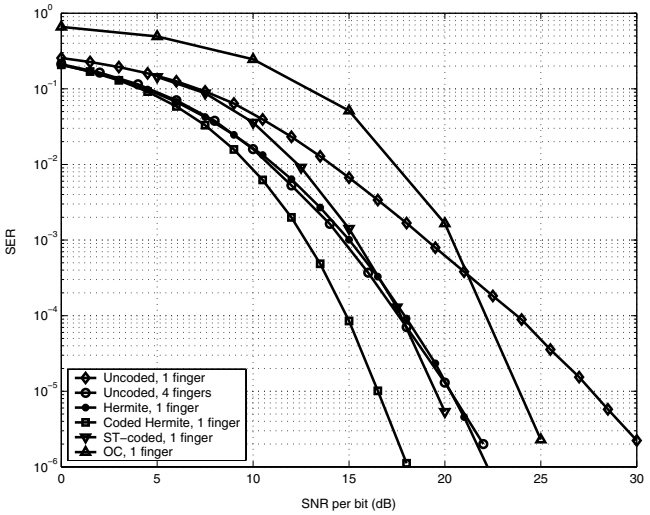

Figure 1: Performance on CM2 at 4 bits PCU with $P = Q = 4$.

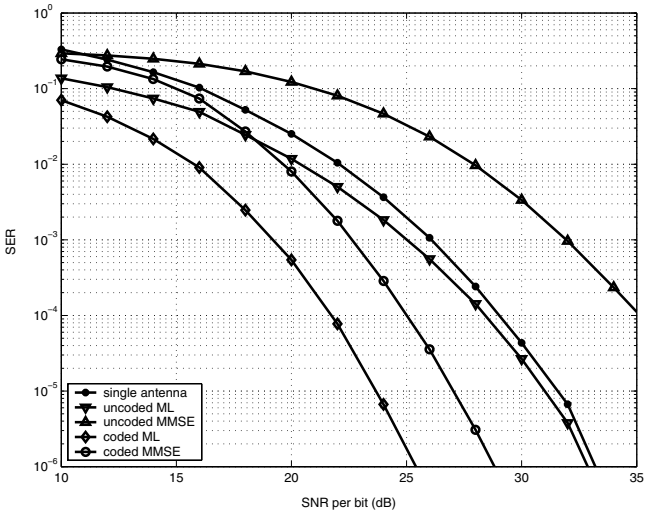

Figure 2: Performance with 8-PPM-8-PAM, $Q = 1$ and $L = 8$.

the average time needed by algorithm j ($j = 0, 1, 2$) to detect one symbol vector. The SNR is fixed at 20 dB and the initial sphere radius is set to infinity. For example, the combined 32-PPM-16-PAM constellation corresponds to a generated lattice with 2^{18} valid points in a 64 dimensional space. In this case, algorithm 1 can "shortcut" up to 31 dimensions and converges 6 times faster than algorithm 0. Results show that algorithm 2 has the best convergence time.

V. Conclusion

In this work, we proposed a new MIMO-UWB scheme that can be a candidate solution for very high data rate systems. Issues related to the encoding and decoding of impulsive pulses were discussed and the proposed system was compared with the existing solutions. Simulations performed over indoor UWB channels showed high performance levels with a moderate complexity.

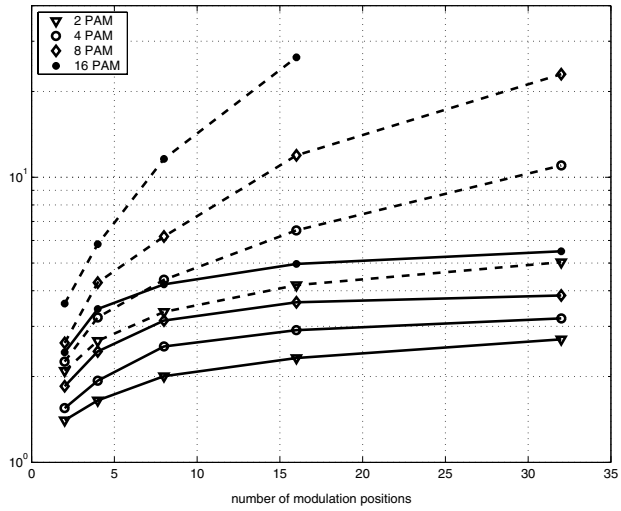

Figure 3: Solid and dashed lines correspond to algorithm 1 and algorithm 2 respectively.

References

[1] H. El Gamal and M. O. Damen, "Universal space-time coding," *IEEE Trans. Inform. Theory*, vol. 49, pp. 1097–1119, May 2003.

[2] F. Oggier, G. Rekaya, J.-C. Belfiore, and E. Viterbo, "Perfect space time block codes," *IEEE Trans. Inform. Theory*, submitted for publication.

[3] J.-C. Belfiore and G. Rekaya, "Quaternionic lattices for space-time coding," in *Proceedings IEEE Information Theory Workshop*, vol. 2, April 2003, pp. 267–270.

[4] M. Weisenhorn and W. Hirt, "Performance of binary antipodal signaling over the indoor UWB MIMO channel," in *Proceedings IEEE International Conference on Communications*, vol. 4, May 2003, pp. 2872–2878.

[5] E. Baccarelli, M. Biagi, C. Pelizzoni, and P. Bellotti, "A novel multi-antenna impulse radio UWB transceiver for broadband high-throughput 4G WLANs," *IEEE Commun. Lett.*, vol. 8, pp. 419 – 421, July 2004.

[6] E. Baccarelli, M. Biagi, and C. Pelizzoni, "A simple multiantenna transceiver for ultra wide band based 4GWLANs," in *IEEE Wireless Communications and Networking Conference*, March 2004, pp. 1782 – 1787.

[7] L. Yang and G. B. Giannakis, "Analog space-time coding for multi-antenna ultra-wideband transmissions," *IEEE Trans. Commun.*, vol. 52, pp. 507–517, March 2004.

[8] C. Abou-Rjeily, N. Daniele, and J.-C. Belfiore, "Space time coding for multiuser ultra-wideband communications," *IEEE Trans. Commun.*, accepted for publication.

[9] H. Harada, K. Ikemoto, and R. Kohno, "Modulation and hopping using modified Hermite pulses for UWB communications," in *joint UWBST and IWUWBS*, May 2004, pp. 336–340.

[10] W. Hu and G. Zheng, "Orthogonal Hermite pulses used for UWB M-ary communication," in *IEEE International Conference on Information Technology Coding and Computing*, April 2005, pp. 97–101.

[11] E. Bayer, F. Oggier, and E. Viterbo, "New algebraic constructions of rotated $\mathbb{Z}^n$ lattice constellations for the Rayleigh fading channel," *IEEE Trans. Inform. Theory*, vol. 50, pp. 702–714, April 2004.

[12] J. Foerster, "Channel modeling sub-committee report final," *IEEE* 802.15-02/490.

[13] E. Viterbo and J. Boutros, "A universal lattice code decoder for fading channels," *IEEE Trans. Inform. Theory*, vol. 45, pp. 1639–1642, July 1999.

[14] M. O. Damen, H. El Gamal, and G. Caire, "On maximum-likelihood detection and the search for the closest lattice point," *IEEE Trans. Inform. Theory*, vol. 49, pp. 2389–2402, October 2003.